Journal of Power Sources 205 (2012) 157–163

Contents lists available at SciVerse ScienceDirect

Journal of Power Sources

journal homepage: www.elsevier.com/locate/jpowsour

Dense yttria-stabilised zirconia electrolyte layers for SOFC by reactive magnetron sputtering

R. Nédélec[a,*], S. Uhlenbruck[a], D. Sebold[a], V.A.C. Haanappel[b], H.-P. Buchkremer[a], D. Stöver[a]

[a] Forschungszentrum Jülich GmbH, Institute of Energy and Climate Research (IEK-1), 52425 Jülich, Germany
[b] Forschungszentrum Jülich GmbH, Institute of Energy and Climate Research (IEK-3), 52425 Jülich, Germany

ARTICLE INFO

Article history:
Received 21 November 2011
Received in revised form 3 January 2012
Accepted 4 January 2012
Available online 12 January 2012

Keywords:
SOFC
Ion-assisted PVD
Physical vapour-phase deposition
8YSZ
Thin electrolyte layers

ABSTRACT

The morphology of layers of fully yttria-stabilised zirconia (YSZ) deposited by reactive magnetron sputtering was studied with regard to their application as thin electrolytes for solid oxide fuel cells (SOFC). A thin layer of YSZ was deposited on top of anode substrates for SOFC. The substrate comprises the warm-pressed anode itself, which supports the complete cell, and an anode functional layer deposited by vacuum slip casting, which is in direct contact with the electrolyte. From previous experiments it is known that non-assisted reactive DC magnetron sputtering produces layers with rather high leak-rate even when depositing at high temperatures. Residual pores on the substrates' surfaces are responsible for the incomplete coverage by the thin electrolyte and are detrimental to the cell's performance. In the present paper, the effect of increasing bias power applied to the substrate is studied. A clear improvement of the layer morphology and gas-tightness can be observed with increasing bias power. SOFC single cell-tests show an improved performance with regard to standard wet-ceramic processing routes.

1. Introduction

The efforts to increase the performance, longevity and reliability of solid oxide fuel cells (SOFC) have led to a stepwise reduction of the operating temperature from the high temperature range between 900 and 1000 °C to the intermediate temperature range of 600–800 °C. One advantage of this approach is that the use of high-temperature ferritic steel alloys has become possible [1–5]. However, the performance of SOFC based on fully yttria-stabilised zirconia (YSZ) electrolytes is strongly limited by the diffusion process of oxygen ions below 800 °C [6]. As a result various efforts have been undertaken to compensate the decrease in performance. The use of other materials is one option. Another more straightforward approach is to reduce considerably the thickness of the YSZ electrolyte layer.

Depositing gas-tight electrolyte layers with a highly uniform thickness has proven challenging [7,8]. Wet-ceramic processing like tape casting and vacuum slip casting or screen-printing result in a layer thickness of 7 μm or higher for anode-supported cells. Calculations show that this is not enough to compensate the losses encountered by the reduced operating temperature [6]. An additional reduction by about one order of magnitude to less than 1 μm is necessary for a decent performance at 600 °C.

Physical vapour phase deposition techniques (PVD) are known for their extremely high reliability and reproducibility. Their main drawback – low deposition rates – can be turned into an advantage here. Highly uniform layer thicknesses well below 500 nm can be achieved on substrates of considerable size. A concern remains nevertheless: depositing such thin layers requires substrates with a very high surface quality. Pores in the substrate's surface reveal to be the most challenging and often require a surface-treatment prior to the PVD deposition [8]. Fig. 1 shows SEM images of anode substrates before and after the deposition of a 1 μm thin electrolyte layer by PVD. The pores present in these substrates are ~3(1) μm in diameter in average and cannot be covered completely, thus, degrading the electrolyte's gas-tightness.

It is reported in the literature that bias-assisted sputtering is capable of producing films with better quality compared to normal sputtering [9]. The bias voltage alters the distribution of the potential in the plasma, turning the substrate into a secondary target. Positively charged Argon atoms are accelerated towards the substrate, eventually hitting its surface. The nucleation process is strongly affected by this particle bombardment: if the Argon atoms have too little kinetic energy their effect will be minor. In the opposite case, when their energy is too high material will be sputtered off the sample's surface. Under optimum conditions, the Argon atoms will provide the necessary displacement energy to enhance the growth process towards layer growth. Thus, using bias the morphology of the deposited layer can be changed from porous to dense. It is for instance reported that by optimising bias settings it

* Corresponding author.
E-mail address: nedelec@hiskp.uni-bonn.de (R. Nédélec).

0378-7753/$ – see front matter © 2012 Elsevier B.V. All rights reserved.
doi:10.1016/j.jpowsour.2012.01.054

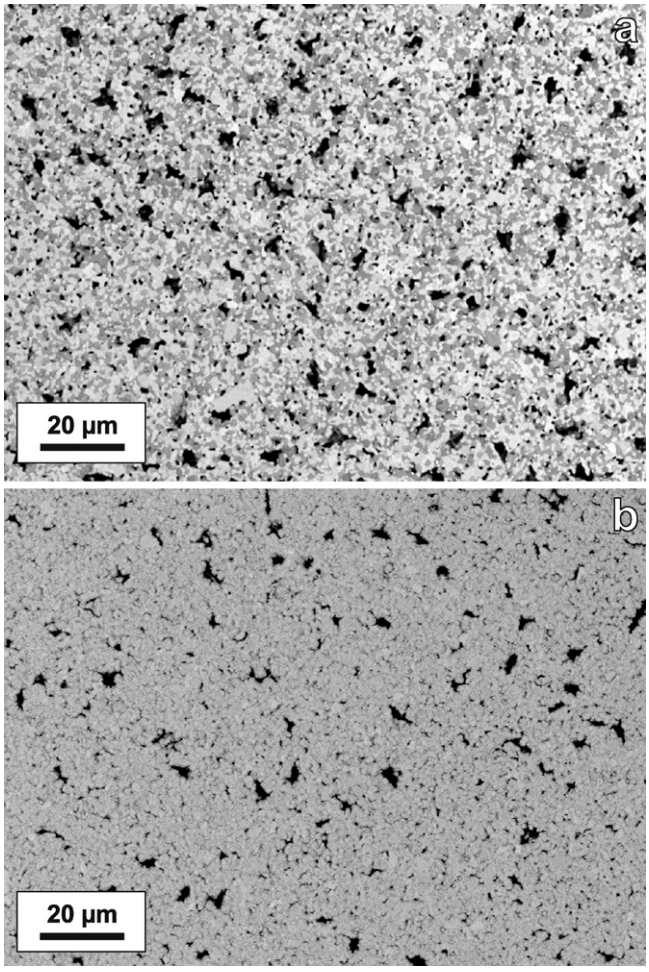

Fig. 1. SEM surface image (backscattered electrons) of an uncoated anode cermet (a). The pores with an average diameter of 3(1) µm cannot be covered by applying a thin electrolyte layer by PVD on top (b).

is possible to increase the electrical conductivity of sputtered films up to the point of bulk conductivity values.

In general, another interesting prospect of bias assistance use is that substrate temperature during deposition can be lowered by a few hundred Kelvin while still achieving a similar result as for unassisted PVD. Besides the advantage of speed there is also a clear economic interest in improving energy consumption. Last but not least, lower processing temperatures allow for the use of temperature sensitive substrates.

In the present study the effect of the applied bias voltage during the sputtering of YSZ layers on warm-pressed anode substrates with anode functional layer was studied. The present work was triggered by the appealing success with the deposition of layers of Gadolinium doped Ceria that serve as diffusion barrier layers for high-performance cathodes composed of (La,Sr)(Co,Fe)$O_{3-\delta}$ [10].

2. Experimental

Anode substrates made of NiO/YSZ were prepared by warm pressing. A ~15 µm thick anode functional layer was then applied by vacuum slip casting. The half-cell substrates were fabricated following the procedures developed at the Forschungszentrum Jülich and further details regarding cell fabrication can be found in the literature [11,12]. After this, samples were cut to dimensions of ~50 mm × 50 mm using a rotating diamond blade saw.

Coatings were carried out in a CS 400ES PVD cluster system (Von Ardenne Anlagentechnik GmbH, Germany). Before deposition substrates were cleaned using organic solvents. After that sputter etching was applied to condition the surface (0.7 W cm^{-2}, 1200 s). Without breaking vacuum the samples were then transferred into the processing chamber and heated up to the deposition temperature of 800 °C at a controlled rate of 300 K h^{-1}.

YSZ coatings were applied by reactive DC magnetron sputtering (RMS). The metallic target made of zirconium is doped with 8 mol.% of yttrium to obtain the desired stoichiometry. Under addition of 8 standard cubic centimetres per minute (sccm) of oxygen during deposition chamber pressure was stabilised at 6×10^{-1} Pa. The DC sputtering power was fixed at ~1.00 W cm^{-2} whereas the RF bias power varied from 0 to 0.5 W cm^{-2}. In an effort to achieve similar layer thicknesses around 1 µm, the deposition time was adapted. The distance between sputtering target and substrate was approximately 55 mm during depositions.

Fractured cross sections and surfaces of the deposited layers were prepared for electron microscopy. A field emission gun scanning electron microscope (FEG-SEM, Zeiss Ultra 55, IncaEnergy 355) allowed microstructural analysis using both back scattered and secondary electrons. The layer composition has been analysed by energy dispersive X-ray spectroscopy (EDS). Additional analysis was performed with an FEI Phenom SEM microscope.

The topographic analysis of the surface of the specimens was performed using a CT-200 laser topographer (cyberTECHNOLOGIES GmbH, Germany) in combination with a confocal laser sensor LT-9010 (Keyence Corp., Japan) delivering a maximum resolution of 2 µm in plane and 0.01 µm in the *z*-axis. The roughness values were calculated according DIN EN ISO 4288 and 3274. Topographic imaging was realised using a VK-9700 confocal laser microscope (Keyence Corp., Japan).

The gas-tightness of the electrolyte layer was evaluated using the pressure increase method. Samples were mounted on the flange of a vacuum chamber with a known volume using an o-ring seal. After evacuating the volume to about 1 Pa the pumping system was disconnected. The leak-rate was then derived from the pressure rising slowly in the chamber. For reference a polished plate made of plain steel was measured. Samples prepared for the evaluation of the electrochemical performance were tested using a commercial Helium leak detection system (QualyTest HLT260, Pfeiffer Vacuum, Germany).

For the single cells tests at least two nominally identical cells were measured. For comparison with SOFC with electrolytes deposited by vacuum slip casting, YSZ was deposited on a batch of five identical 50 mm × 50 mm cells using 0.5 W cm^{-2} bias-power. All of the samples for the evaluation of electrochemical performance were provided with a diffusion barrier layer of Gadolinia-doped Ceria ($Ce_{0.8}Gd_{0.2}O_{2-\delta}$, GDC) before applying the cathode. It was sputtered in a similar way like the YSZ layers described previously [8]. The dimensions of this barrier layer were set to cover the whole surface of the cells with PVD electrolytes, in order to further improve their gas-tightness.

Finally, a cathode made of $La_{0.58}Sr_{0.4}Fe_{0.8}Co_{0.2}O_{3-\delta}$ (LSFC) powder by using conventionally prepared ceramic suspensions was screen printed onto the GDC interlayer. Details concerning the preparation of both LSFC powder and suspension are reported elsewhere [8,13]. After the screen-printing depositions covering a 40 mm × 40 mm area of the single cells, these were first dried in hot argon atmosphere for 1 h, and then fired at 1040 °C for 3 h in air. The final thickness of cathode layer was around 50 µm. For reference half-cells with a 10 µm thick vacuum-slip-casted electrolyte were coated with the same cathode paste.

The electrochemical performance was tested after sealing the cells in an alumina housing using a gold sealant, which then were placed in a resistive furnace [13,14]. The electrical contact was

Table 1
The roughness of the substrates surface was measured by confocal laser topography before and after the deposition of 8YSZ layers by reactive magnetron sputtering.

	R_a [μm]	R_q [μm]	R_z [μm]	R_{max} [μm]
Uncoated surface	0.37(2)	0.47(2)	2.4(1)	2.9(1)
8YSZ without bias	0.47(2)	0.60(3)	3.1(2)	4.0(2)
8YSZ with bias	0.50(3)	0.65(3)	3.4(2)	4.8(2)

realised by a Ni mesh on the anode side and a Pt mesh on the cathode side. After the controlled reduction of the anode, hydrogen (3 vol.% H_2O) was flown into the chamber at 1000 ml min^{-1} using mass flow controllers. Polarisation curves were collected by direct current measurements using a current-control power supply of the type Gossen 62N-SSP500-40 (Gossen-Metrawatt GmbH, Germany), and a computer-controlled data acquisition system.

3. Results and discussion

The microstructure of the sputtered YSZ electrolyte layers deposited on anode substrates with anode functional layers at 800 °C was investigated using a FEG-SEM. Figs. 2 and 3 show micrographs taken from surfaces and from cross-sections.

The micrographs for the deposition without bias assistance (Figs. 2a and 3a) show already very good layer thickness homogeneity, which is typical for PVD. Yet layer growth is columnar, which can be explained by the initial island growth of the YSZ on the anode functional layer materials NiO and YSZ. The islands do not attain the coalescence stage completely, thus, limiting the continuity of the deposited layer [9]. A similar behaviour can also be observed for other ceramic materials sputtered [10]. These discontinuities have a clear negative effect on gas-tightness of layers as will be discussed below.

Increasing the applied bias power progressively changes the microstructural properties of the YSZ electrolyte layers. At 0.1 W cm^{-2} bias power columnar growth is still clearly visible (Figs. 2b and 3b). The coarsening of the columns seen in the cross-section micrograph can also be found in the corresponding picture of the surface. Despite a slight reduction in confront to the unassisted deposition plenty of cracks and pores can still be found between the grains. It is important to notice that already this rather low bias setting is pushing YSZ material towards pores and cracks, thereby effectively reducing the extent of the non gas-tight area. Further increasing bias power to 0.3 W cm^{-2} changes the layer microstructure completely. The fraction in Fig. 3c shows no more signs of columnar growth. In contrast to Fig. 2a, where the surface reproduces the underlying grain structure with its pores and cracks closely, the layer in Fig. 2c is already nearly defect free.

Finally, increasing the bias power even more to 0.5 W cm^{-2} (Figs. 2d and 3d) results in an irregular microstructure of the layer. Columnar type growth is visible only on very short range within the layer, then interrupted and starting over again. A possible explanation for this is that the nucleation process is strongly disturbed by the energetic ion bombardment: If some part of the area of the surface becomes amorphous during deposition, the nucleation process has to start over. This then leads to the observed interruption of the columnar structures present in that area at that time. In contrast, the surface image shows a dense, continuous layer very similar to the 0.3 W cm^{-2} deposition. Yet, a few noticeable differences deserve attention.

Laser-topographic scans of these different samples are compared in Fig. 4. The corresponding values for the surface roughness are compiled in Table 1. R_a is the arithmetic average roughness, whereas R_q, R_z and R_{max} are the RMS average roughness, the mean roughness depth and the maximum roughness depth, respectively. All the samples shown in Figs. 2 and 3 were cut from the same

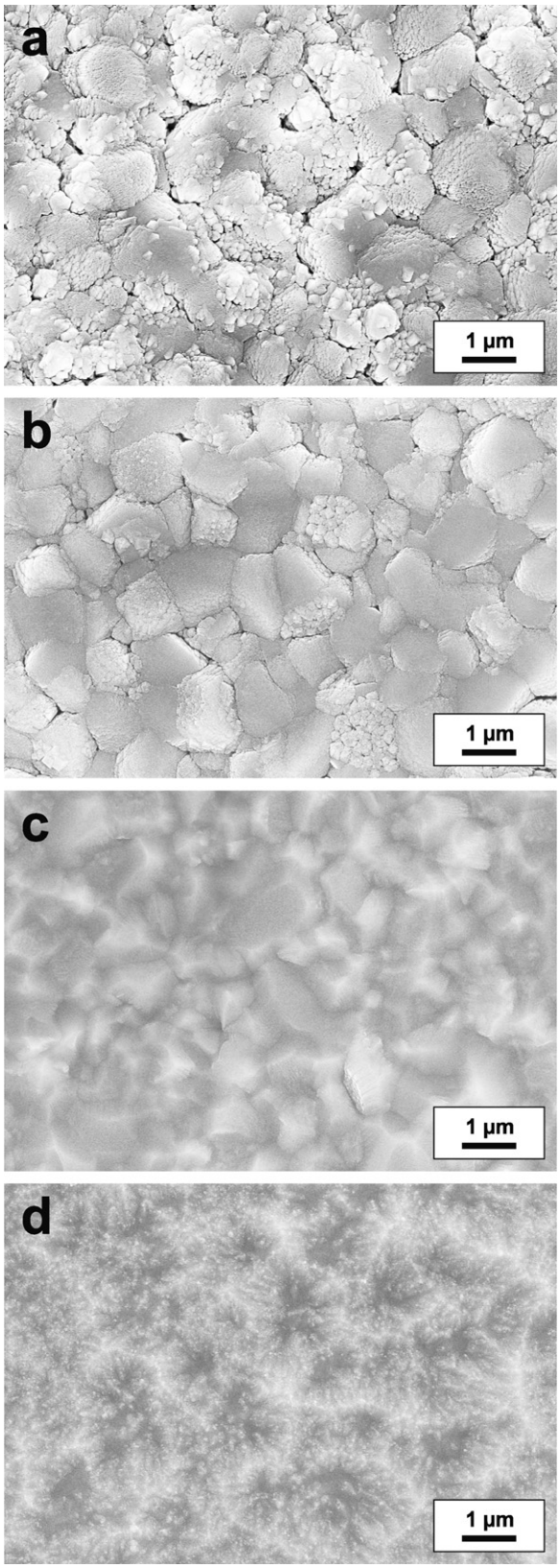

Fig. 2. SEM surface pictures of YSZ layers sputtered using increasing bias power on ceramic anode substrates (in-lens secondary electron detector). Different settings for the bias-power were tested: no bias (a), 0.1 W cm^{-2} (b), 0.3 W cm^{-2} (c) and 0.5 W cm^{-2} (d). The drastic effect of bias on layer morphology and density is clearly visible.

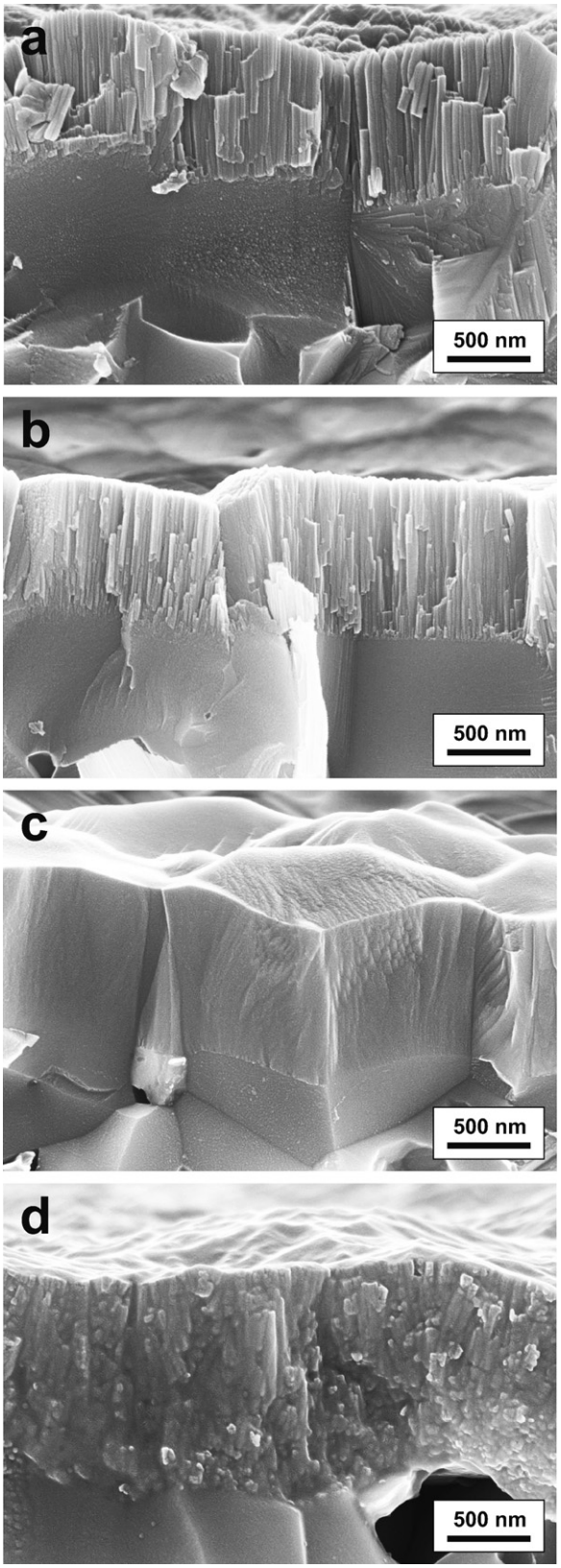

Fig. 3. The SEM pictures of the cross-sections show the impact on the layer growth (in-lens secondary electron detector). The columnar growth typical for PVD is observed without bias (a). With increasing bias – 0.1 W cm^{-2} (b), 0.3 W cm^{-2} (c) and 0.5 W cm^{-2} (d) – this columnar growth is more and more suppressed. A denser morphology is observed instead.

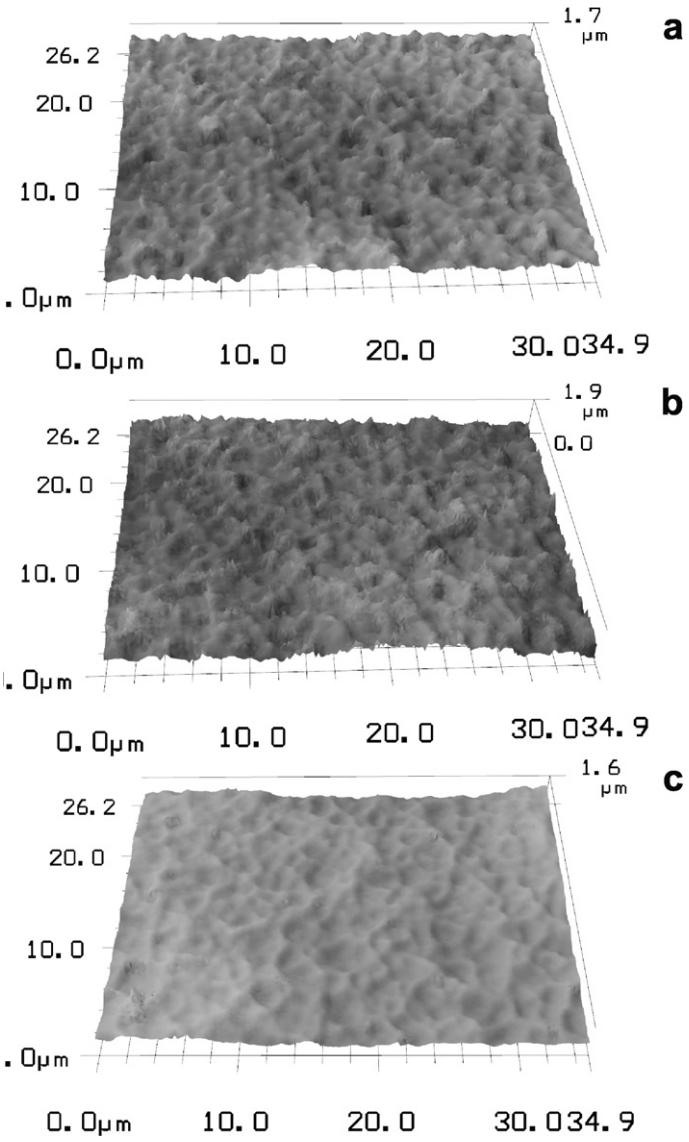

Fig. 4. Laser-topographic imaging of the surface of samples prior to deposition (a), deposited without bias assistance (b) and using 0.5 W cm^{-2} (c) bias-power. In addition to changing the morphology of the deposited layer, the bombardment with Argon ions also affects the roughness of the underlying substrate.

original 200 mm × 200 mm substrate. The uncoated substrate has a rather rough surface morphology. The uncoated surface and the surface of the sample coated without bias have a similar surface topography. The PVD layer is thin with regard to the roughness of the underlying substrate and, therefore, reproduces its surface quite well. Applying bias during deposition visually smoothes the surface out. The analysis of the roughness does not coincide with the optical impression. A moderate increase is found for the coated samples (without bias R_a = 0.47(2) µm, R_z = 3.1(2) µm, with bias R_a = 0.50(3) µm, R_z = 3.4(2) µm) with regard to the uncoated (R_a = 0.37(2) µm, R_z = 2.4(1) µm). This is due to the fact, that the surface roughness as defined by the norm only takes into account the height difference and does not reflect the rippling/wavelength of the oscillations of the surface.

The particle bombardment of the substrate's surface during reactive magnetron sputtering with bias assistance influences the resulting layer thickness. If deposition time is kept constant a decrease in layer thickness is expected. Fig. 5 plots the dependence of the ratio of layer growth rate against bias power density as found. Layer thickness was averaged from values measured at

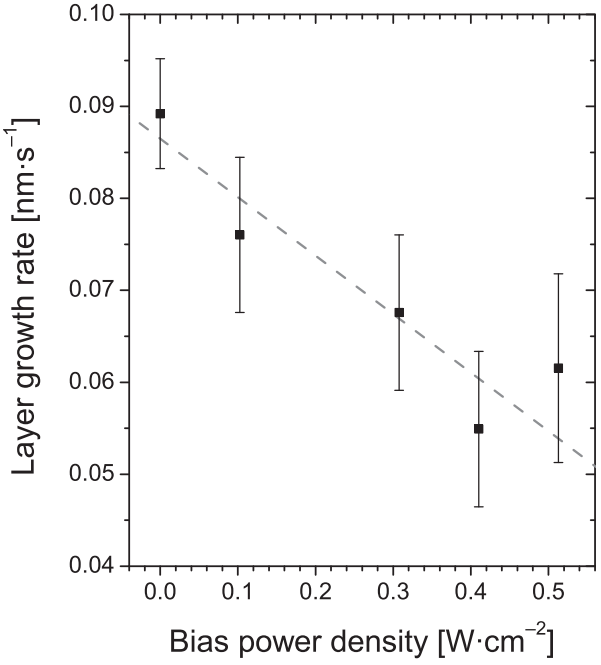

Fig. 5. The particle bombardment of the substrate's surface influences the total layer growth rate. The plot shows the ratio of layer growth-rate and DC bias power density. With increasing bias power density it is reduced to about 2/3 of its original value without ion assistance.

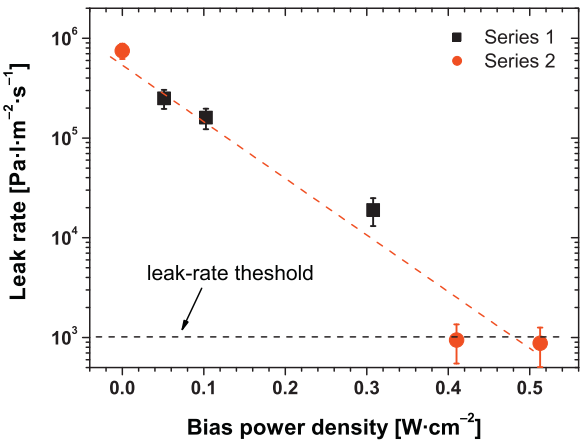

Fig. 6. Leak-rates for samples cut from the same original substrate, coated with different settings for the applied bias-power. With increasing bias-power density the leak-rate improves by several orders of magnitude, dropping from 7.5×10^5 Pa l m^{-2} s^{-1} without bias-assistance down to $\sim 9 \times 10^2$ Pa l m^{-2} s^{-1} at 0.4 or 0.5 W cm^{-2}. Randomly distributed larger defects on the substrate's surface have a measurable impact on the leak-rate, leading to some scattering of the data. The horizontal dashed line indicates the minimum requirements for electrochemical performance testing.

$\sim$10 different spots along the cross-sections. The deposition rate for YSZ at 800 °C drops from 87(8) pm s^{-1} without bias assistance to $\sim$57(9) pm s^{-1} for bias-power above 0.4 W cm^{-2}. Two explanations exist for this: on the one hand, particles that are already attached to the substrate's surface get sputtered away instead of being covered. This reduces the amount of material deposited on the surface. On the other hand, deposited layers are denser (see Figs. 2 and 3). The same amount of material being packed into a smaller volume leads to thinner layers if area remains unchanged [9].

One important criterion for the quality of an electrolyte layer is its gas-tightness. In order to avoid the uncontrolled thermal combustion of hydrogen in the fuel cell a threshold of about 10^3 Pa l m^{-2} s^{-1} (10^{-3} mbar l cm^{-2} s^{-1}) must not be exceeded [11]. Leak-rates were measured using the rising pressure method on samples coated with different settings for the bias power. Fig. 6 summarises the results. Electrolyte layers sputtered without bias assistance miss the requirements by far. This has already been observed in previous work [8]. Increasing bias-power to 0.05 or 0.1 W cm^{-2} only betters leak-rate slightly. Coinciding with the complete change of the layer morphology from columnar to dense observed in Figs. 2 and 3 with 1.9×10^4 Pa l m^{-2} s^{-1} the leak-rate considerably improves for bias settings of 0.3 W cm^{-2}. Further increasing the bias-power to 0.4 and 0.5 W cm^{-2} again reduces the leak-rate by more than one order of magnitude to $\sim 9 \times 10^2$ Pa l m^{-2} s^{-1}. Interestingly, no noticeable difference is seen between the depositions for 0.4 and 0.5 W cm^{-2}, and this holds even though the layer thickness of the electrolyte was increased from $\sim$0.7 μm to about 1.2 μm. Since SEM images show a similar layer morphology for these depositions, it can be concluded that an optimum bias setting with regard to gas-tightness is found and further increasing bias power will only lead to a reduced deposition rate.

Five substrates similar to the first series were sputtered with YSZ using 0.5 W cm^{-2} of bias-power. Before screen-printing the cathodes the leak-rates of the half-cells were confirmed. Lying between 1 and 4×10^2 Pa l m^{-2} s^{-1}, all prepared cells met the requirements for evaluating their electrochemical performance. The measured values hold for a bi-layer composed of the actual electrolyte and a diffusion barrier layer made of GDC. The polarisation curves shown in Fig. 7 were measured in the temperature range between 600 and 850 °C. The open-circuit voltage around 1.1 V is as expected by the Nernst equation and confirms that the PVD electrolyte layer is sufficiently gas-tight. Aside that, the cells show a typical behaviour for SOFC under load: The performance of the cells drastically increases with increasing operating temperature. This behaviour occurs, because different effects contribute to the cell's electric resistance. As the polarisation losses at the interfaces (e.g. the 8YSZ-GDC layer transition) vary only very little, the bulk ohmic resistance of the layers becomes increasingly significant at lower temperatures. Raising the operating temperature above 800 °C does not lead to a higher power output. More than one explanation exists for this effect. One reason is that the advantage of high catalytic activity of LSCF becomes minor important at higher temperature. Another possible reason is an increasing leak-rate at higher temperatures due to micro-cracks in the very thin electrolyte layer in combination with the thermal expansion of the cell.

The over-all performance of the reference cells at operating temperatures above 800 °C is to some extent inferior to state-of-the-art anode supported SOFC (Jülich mean value 2005–2008, see Fig. 8a). Below 800 °C the observed performance is superior to the average state-of-the-art cells. The superiority of the PVD electrolyte layers becomes clearly evident below 650 °C. At 600 °C SOFCs with PVD electrolytes out-run conventionally produced SOFCs ($\sim$0.3 A cm^{-2}

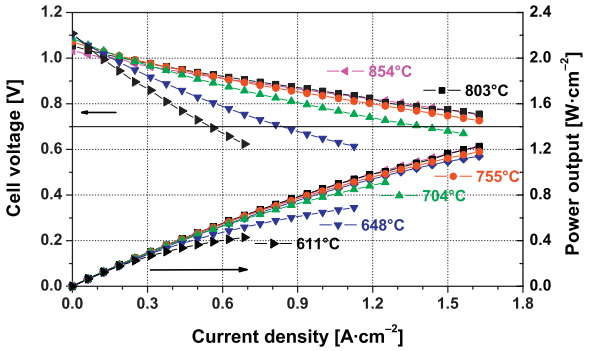

Fig. 7. Electrochemical performance data for cells based on warm-pressed substrates with an anode functional layer and with a PVD electrolyte layer.

Table 2
Comparison of the mean ASR values measured for fuel cells with a PVD electrolyte (present work) and fuel cells with a conventional electrolyte applied by vacuum slip casting (VSC). Due to the poor performance of cells with VSC electrolytes reliable measurements are not possible at 600 °C.

Operating temperature [°C]	ASR single cell with PVD electrolyte [mΩ cm^2]	ASR single cell with VSC electrolyte [mΩ cm^2]
600	640(64)	–
650	396(52)	470(15)
700	228(36)	263(9)
750	175(9)	201(5)
800	160(8)	167(3)
850	165(13)	149(3)
900	163(18)	146(4)

at 700 mV) by delivering approx. 65% more power. Calculations confirm that this dramatic performance increase can be directly linked to the thickness of the 8YSZ electrolyte layer [6,8]. In accordance with the performance increase a drop of the total area specific resistance (ASR) of the cells is observed (Fig. 8b, Table 2). This behaviour is mainly due to the diffusion process of oxygen ions through the electrolyte, which depends exponentially on the temperature. As expected, for higher operating temperature the difference to conventionally produced SOFCs is minimal. At 600 and 650 °C a net progress is seen. At 650 °C the ASR values are comparable: around 470(15) mΩ cm^2 for standard cells and 400(50) mΩ cm^2 for the cells with a PVD electrolyte. At 600 °C the ASR cannot be determined for standard cells due to their insufficient performance. The cells with a PVD-electrolyte, however, can be measured. The averaged ASR observed lies at 640(64) mΩ cm^2.

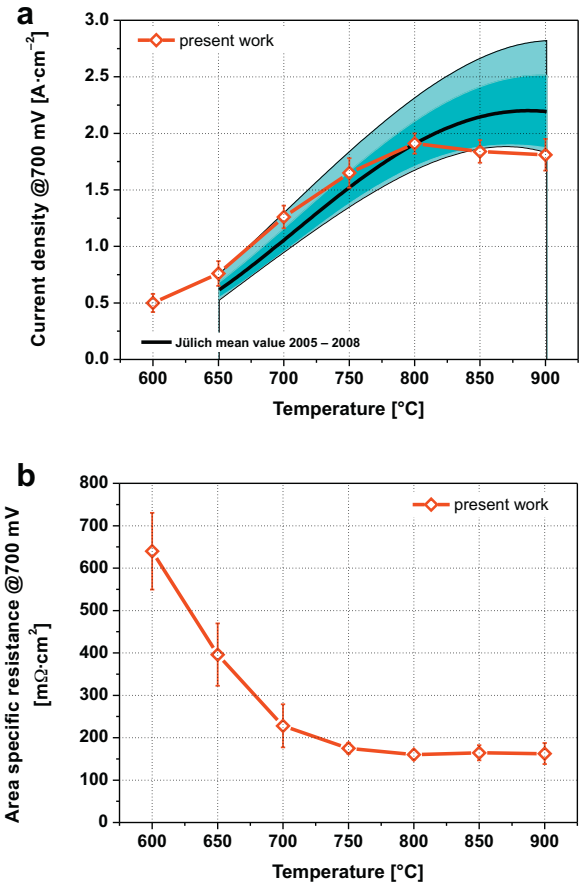

Fig. 8. (a) Comparison of the average output current density at 700 mV of standard cells with electrolyte layers by vacuum slip casting (VSC) and cells with a PVD electrolyte as a function of temperature. (b) Corresponding values for the area specific resistance (ASR) for the cells with PVD electrolytes. The coloured ribbon marks the average power output observed for cells with VSC electrolytes in Jülich.

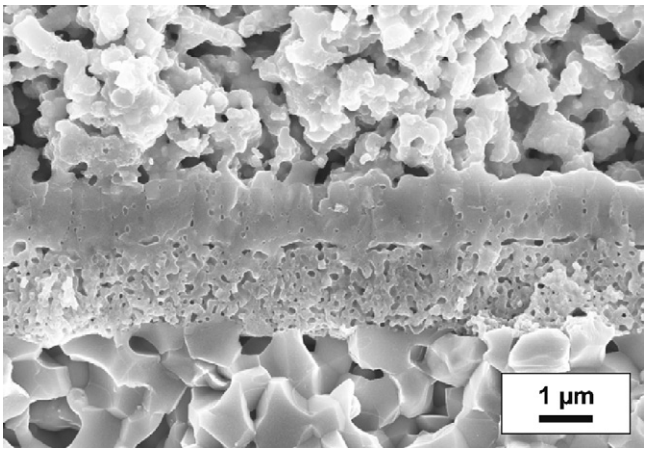

Fig. 9. SEM polished cross-section of the ~1 µm thick electrolyte and the diffusion barrier layer (on top) of a cell with a PVD electrolyte taken after the electrochemical performance testing (in-lens secondary electron detector).

Fig. 9 compares SEM pictures taken from a polished cross-section after the cell-test. The morphology of the GDC-layer has been altered by sintering effects, but remains rather dense. The changes are more pronounced for the YSZ-layer underneath, where in addition a fairly large amount of closed porosity is found. The morphology change can be attributed to the substrate temperature during deposition (800 °C) and the sintering temperature of the cathode (1040 °C). According to Movchan, Demchishin [15], and Thornton [16], the morphology of a ceramic layer deposited by PVD is linked to the ratio between deposition temperature and melting temperature of the deposited material. At the present deposition temperature both GDC and YSZ exhibit columnar growth. This implies the presence of small inter-columnar gaps, which lead to an inherent porosity of the layer. The melting temperature for YSZ is considerably higher than for GDC, thus, explaining the higher inherent porosity of the YSZ-layer. However, it can be concluded that the formation of this closed porosity during post-deposition sintering of the PVD-layers does not lead to a discontinuity of the electrolyte and therefore does not affect the gas-tightness or the performance of the cell.

4. Conclusions

Bias assistance turns out to be a very powerful tool to enhance the properties of YSZ electrolyte layers for SOFC deposited by reactive DC magnetron sputtering. The use of bias allows the change of the layer growth morphology from columnar to a denser structure. In particular, gas-tight electrolyte layers could be deposited by PVD on to anode substrates without the need of any antecedent special surface treatment or coating. Avoiding additional processing steps prior to electrolyte deposition is a significant advance for the application of PVD technology in SOFC. Also, the use of bias during deposition effectively prevents the formation of cracks in the

electrolyte layer during post-deposition heat treatment at temperatures significantly above deposition temperature, which are e.g. required for cathode sintering.

Furthermore, it could be shown that cells with PVD electrolytes perform as well as cells with vacuum-slip-casted electrolyte layers for operating temperatures between 700 and 850 °C. Below 700 °C the only less than 1 μm thick PVD electrolyte leads to a clear increase of the performance. This effect is due to the reduction of the area specific resistance of the electrolyte layer, which becomes decisive in that temperature range as discussed.

Acknowledgements

The authors wish to thank F. Vondahlen, W. Herzhof and K. Portulidou for their respective help with the PVD depositions and for providing anode substrate material and cathode depositions.

References

[1] J.W. Fergus, Mat. Sci. Eng. A397 (1–2) (2005) 271–283.
[2] J.W. Fergus, Solid State Ionics 171 (1–2) (2004) 1–15.
[3] ThyssenKrupp VDM GmbH, Product data sheet for Crofer 22 APU.
[4] F.J. Pirón Abellán, W.J. Quadakkers, Development of Ferritic Steels for Application as Interconnect Materials for Intermediate Temperature Solid Oxide Fuel Cells (SOFCs), Forschungszentrum Jülich GmbH, 2005, JUEL-4170, ISSN: 0944-2952.
[5] W.J. Quadakkers, J. Piron-Abellan, V. Shemet, L. Singheiser, Mater. High Temp. 20 (2) (2003) 115–127.
[6] V.V. Kharton, F.M.B. Marques, A. Atkinson, Solid State Ionics 174 (2004) 135–149.
[7] R. Hui, J.O. Berghaus, C.D. Petit, W. Qu, S. Yick, J.G. Legoux, C. Moreau, J. Power Sources 191 (2009) 371–376.
[8] N. Jordan, Doctor Thesis, Herstellung von Hochtemperatur-Brennstoffzellen über physikalische Gasphasenabscheidung, Forschungszentrum Jülich GmbH, ISBN 978-3-89336-565-4 (2008).
[9] B.N. Chapman, Glow Discharge Processes: Sputtering and Plasma Etching, John Wiley and Sons, New York, 1980.
[10] F.C. Fonseca, S. Uhlenbruck, R. Nédélec, H.P. Buchkremer, J. Power Sources 195/6 (2010) 1599–1604.
[11] H.P. Buchkremer, U. Diekmann, D. Stöver, Components manufacturing and stack integration of an anode supported planar SOFC system, in: Proceedings of 2nd European Solid Oxide Fuel Cell Forum, 1996, p. 221.
[12] F. Tietz, Q. Fu, V.A.C. Haanappel, A. Mai, N.H. Menzler, S. Uhlenbruck, Int. J. Appl. Ceram. Technol. 4 (2007) 436–445.
[13] S. Uhlenbruck, N. Jordan, D. Sebold, H.P. Buchkremer, V.A.C. Haanappel, D. Stöver, Thin Solid Films 515 (2007) 4053–4060.
[14] N. Jordan, W. Assenmacher, S. Uhlenbruck, V.A.C. Haanappel, H.P. Buchkremer, D. Stöver, W. Mader, Solid State Ionics 179 (2008) 919–923.
[15] B.A. Movchan, A.V. Demchishin, Phys. Met. Metallogr. 28 (1969) 83–90.
[16] J.A. Thornton, J. Vac. Sci. Technol. 11 (4) (1974) 666–670.